Influence of the donor size in panchromatic D–π-A–π-A dyes bearing 5-phenyl-5H-dibenzo-[b,f]azepine units for dye-sensitized solar cells

Wang, Yafei; Yang, Chuncheng; Chen, Jue; Qi, Hongrui; Hua, Jianli; Liu, Yu; Baranoff, Etienne; Tan, Hua; Fan, Jiang; Zhu, Weiguo

DOI:
10.1016/j.dyepig.2016.01.004

Accepted Manuscript

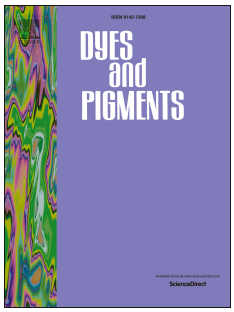

Influence of the Donor Size in Panchromatic D-π-A-π-A Dyes Bearing 5-Phenyl-5*H*-dibenzo-[*b,f*]azepine Units for Dye-Sensitized Solar Cells

Yafei Wang, Chuncheng Yang, Jue Chen, Hongrui Qi, Jianli Hua, Yu Liu, Etienne Baranoff, Hua Tan, Jiang Fan, Weiguo Zhu

PII: S0143-7208(16)00006-1

DOI: 10.1016/j.dyepig.2016.01.004

Reference: DYPI 5056

To appear in: *Dyes and Pigments*

Received Date: 18 August 2015

Revised Date: 3 November 2015

Accepted Date: 4 January 2016

Please cite this article as: Wang Y, Yang C, Chen J, Qi H, Hua J, Liu Y, Baranoff E, Tan H, Fan J, Zhu W, Influence of the Donor Size in Panchromatic D-π-A-π-A Dyes Bearing 5-Phenyl-5*H*-dibenzo-[*b,f*]azepine Units for Dye-Sensitized Solar Cells, *Dyes and Pigments* (2016), doi: 10.1016/j.dyepig.2016.01.004.

Influence of the Donor Size in Panchromatic D-π-A-π-A Dyes Bearing 5-Phenyl-5*H*-dibenzo-[*b*,*f*]azepine Units for Dye-Sensitized Solar Cells

Yafei Wang†‖[*], Chuncheng Yang†&, Jue Chen‡&, Hongrui Qi†, Jianli Hua‡, Yu Liu†, Etienne Baranoff[Δ], Hua Tan†, Jiang Fan†, Weiguo Zhu†[*]*

†*College of Chemistry, Key Lab of Environment-Friendly Chemistry and Application of the Ministry of Education, Xiangtan University, Xiangtan 411105, China*

‡*Key Laboratory for Advanced Materials and Institute of Fine Chemicals, East China University of Science and Technology, 130 Meilong Road, Shanghai 200237, PR China*

[Δ] *School of Chemistry, University of Birmingham, B15 2TT UK*

‖*Institute of Polymer Optoelectronic Materials and Devices, State Key Laboratory of Luminescent Materials and Devices, South China University of Technology, Guangzhou 510640, China*

& The authors contributed equally to this work.

*To whom correspondence should be addressed

(E. Baranoff) e.baranoff@bham.ac.uk

(W. Zhu) zhuwg18@126.com

(Y. Wang) wangyf_miracle@hotmail.com

Abstract

Two D-π-A-π-A organic dyes (**YC-1** and **YC-2**) with 5-phenyl-5*H*-dibenzo[*b*,*f*]azepine derivatives as donor, thiophene as π bridge, and isoindigo and cyanoacrylic acid as acceptors were prepared. **YC-1** and **YC-2** show a panchromatic absorption between 300 nm and 800 nm both in solution and neat film. The photovoltaic performances of both dyes were evaluated in dye-sensitized solar cells based on iodide/triiodide electrolyte without any co-sensitizer. The **YC-1** based device displays better device performance with open-circuit photocurrent density of 12.12 mA cm^{-2}, open-circuit voltage of 0.53 V, and fill factor of 68.9 %, corresponding to overall conversion efficiency (η) of 4.38 %. The inferior performance of device based on **YC-2** (η = 1.46 %) is ascribed to short electron life time as evidenced from electrochemical impedance spectroscopy measurement. This research provided a potential promising donor unit for organic dyes and revealed the influence of donor size in organic dyes for photovoltaic performances.

Keywords: 5-phenyl-5H-dibenzo[*b*,*f*]azepine; Isoindigo; D-π-A-π-A framework; Photovoltaic performance; Dye-sensitizer solar cells;

1. Introduction

Dye-sensitized solar cells (DSSCs) have emerged as one promising candidate for renewable and green energy owing to their low cost fabrication procedure and attractive power conversion efficiency (η) [1,2]. To date, a great deal of sensitizing dyes, including metal complexes [3-8] and organic molecules [9-12], has been exploited to achieve high η. As such, several DSSCs show η > 10% under AM1.5 simulated solar light (100 mW cm^{-2}) [13-17]. Compared to ruthenium-based sensitizers, organic dyes are attractive because of their high molar extinction coefficients, structural variety and possibly low cost due to the absence of platinoid ion and exciting progresses have been made recently with these materials [18,19].

Generally, effective organic dyes for high performance of DSSCs are constructed around a donor-π-bridge-acceptor (D-π-A) framework resulting in effective intramolecular charge transfer [20-24]. Recently, the concept has been extended to D-A-π-A [24-29] architecture, in which the additional acceptor unit is favorable to the photophysical properties of the dyes, enhancing the photovoltaic performances and the photostability of dyes. Among these DSSCs dyes, considerable endeavors have been made to design new-type donor moieties, such as triphenylamine [10,19,25], carbazole [23,24], phorphyrin [26], indoline [30] and phthalocyanine derivatives [31,32]. Triarylamine derivatives are the one of most effective dyes in DSSCs owing to their good electron-donating character and generally reversible oxidation process [33]. Conversion efficiencies in the range of 9-10 % have been reported with arylamine-based organic dyes [33]. For example, a D-A-π-A dye (WS-9) using

indoline derivatives as the donor, cyanoacrylic acid as the acceptor, n-hexylthiophene unit as the conjugated spacer and the benzothiadiazole unit as the additional acceptor unit achieved η = 9.04% with iodine electrolyte [34]. Hua and coworkers designed an D-A-π-A motif based on arylamine organic dyes utilizing quinoxaline unit as the additional acceptor moiety (YA422), resulting in a η = 10.65% with $[Co(bpy)_3]^{3+/2+}$ electrolyte [35]. However, arylamine-based organic dyes remain some challenges including lack of absorption in the near-infrared region and dye aggregation on the TiO_2 film. Therefore, further red-shifted absorption spectra can be obtained by grafting additional conjugated spacer between the donor and acceptor units to form a D-π-A-π-A framework owing to the expended conjugation. Lin and his coworkers demonstrated the D-π-A-π-A motif possessed broad absorption spectra and efficient light-to-electricity conversions [36]. Even so, the research of structure-property relationship of this D-π-A-π-A motif is still overlooked.

Encouraged by the successful application of triphenylamine (TPA) to DSSCs, herein we propose the use of 5-phenyl-5*H*-dibenzo[*b*,*f*]azepine, PDBAz, as a novel donor group of organic dye for DSSC. Because of some structural similarity with TPA, it was expected that PDBAz would still provide advantageous properties of TPA, such as good hole transporting ability and sterically-hindered structure limiting dye aggregations [37-39]. Furthermore, the additional conjugation in PDBAz would result in red-shifted absorption, thus leading to an expected enhancement of J_{sc}.

We have prepared two dyes based on the D-π-A-π-A architecture with isoindigo and cyanoacrylic acid as acceptor groups and thiophene as π-linker. 2-Ethylhexyl

chains were grafted onto the isoindigo unit to ensure solubility and disrupt undesirable dye aggregation. To study the effect of molecular structure on photovoltaic performance, two donor groups were used: dye **YC-1** has PDBAz while dye **YC-2** uses bis-PDBA-aniline, a much bulkier donor moiety (**Chart 1**). Both dyes show panchromatic absorption from 300 nm to 800 nm in solution and neat film. To study the effect of the donor size on photovoltaic performance, **YC-1** and **YC-2** were used as sensitizer for dye-sensitized solar cells with an iodide-based electrolyte. The device using **YC-1** as the sensitizer exhibited better photovoltaic performance (η = 4.38% with J_{sc} = 12.12 mA cm^{-2}) than the cell using **YC-2** (η = 1.46% with J_{sc} = 4.84 mA cm^{-2}) due to major difference in J_{SC}. Compared to the analogous TPA-based dye (**ID1**: 3.52 %, 9.89 mA cm^{-2}) [38], **YC-1** shows enhanced performance in the same condition. Density functional theory (DFT) calculations and electrochemical impedance spectroscopy (EIS) have been used to understand the structure-property relationship of both **YC-1** and **YC-2**.

2. Experimental section

2.1. Materials

Transparent conducting oxide (TCO, 15 Ω /square, F-doped SnO_2 from Geao Science and Educational Co. Ltd.) was used as the substrate for the TiO_2 thin-film electrode. Methoxypropionitrile (MPN) was purchased from Aldrich. Tetra-*n*-butylammonium hexafluorophosphate ($TBAPF_6$) and lithium iodide were bought from Fluka. Iodine (99.999%) was purchased from Alfa Aesar. Intermediate **7** has been reported in the

previous literature [40]. The starting material of 10-methoxy-5*H*-dibenzo[*b*,*f*]azepine is purchased from Energy Chemical. All other solvents and chemicals used in this work were of reagent grade and used without further purification.

2.2. **Characterization**

^{1}H NMR and ^{13}C NMR spectra were obtained with a Brucker AM 400 spectrometer. Mass spectra (MS) were recorded on a Bruker Autoflex MALDITOF instrument using dithranol as a matrix. The UV-vis absorption and photoluminescence spectra were measured with a Varian Cray 50. Cyclic voltammograms were performed with a Versastat II electrochemical workstation (Princeton applied research) using a normal three-electrode cell with a Pt working electrode, a Pt wire counter electrode, and Ag/AgCl reference electrode. The photovoltaic characterization was performed on the setup that constitutes a 450 W xenon lamp (Oriel), a Schott K113 Tempax sunlight filter (PräzisionsGlas & Optik GmbH), and a source meter (Keithley 2400) which applies potential bias and measures the photogenerated current. IPCE was obtained using a SR830 lock-in amplifier, a 300 W xenon lamp (ILC Technology) and a Gemini-180 double monochromator (Jobin-Yvon Ltd.). The electrochemical impedance spectroscopy measurements of all the DSSCs were performed using a Zahner IM6e Impedance Analyzer (ZAHNER-Elektrik GmbH & CoKG, Kronach, Germany). The frequency range is 0.1 Hz-100 kHz. The applied voltage bias is from -0.60 V to -0.85 V. The magnitude of the alternating signal is 5 mV. Intensity modulated photovoltage spectroscopy was obtained by the Zahner IM6e Impedance Analyzer (ZAHNER-Elektrik GmbH & CoKG, Kronach, Germany) and a

light-emitting display array (λ = 457 nm, blue light). The frequency range is 0.1 Hz-100 kHz.

2.3. **Fabrication of DSSCs**

Four layers of Dyesol 90-T TiO_2 paste and a scattering layer were screen-printed onto the FTO glass. The photoanodes was sintered gradually up to 500 ^oC and kept at this temperature before cooling. The photoanodes were immersed into 40 mM $TiCl_4$ aqueous solution at 70 ^oC for 30 min and sintered at 450 ^oC for 30 min and cooled down to 80 ^oC. Then the photoanodes were placed into 3×10^{-4} M dye bath in DCM solution for 6 h. The dye-sensitized photoanodes were sealed with platinized counter electrodes by a hot-melt film (25-μm-thick Surlyn, Dupont). The electrolytes were introduced to the cells via two pre-drilled holes in the counter electrodes. The electrolyte consists of 0.05 M I_2, 0.05 M LiI, 0.5 M BMII, 0.1 M DMPII and 0.1 M GuSCN in acetonitrile. The active area of all DSSCs is 0.12 cm^2.

2.4. Synthesis

5-(4-bromophenyl)-10-methoxy-5*H*-dibenzo[*b,f*]azepine (1)

To a solution of 10-methoxy-5*H*-dibenzo[*b,f*]azepine (223 mg, 1.0 mmol), sodium *tert*-butoxide (t-BuONa) (288 mg, 3.0 mmol) and tris(dibenzylideneacetone) -dipalladium ($Pd_2(dba)_3$) (11.6 mg, 0.01 mmol) in dry toluene (15 mL) was added tri-*tert*-butylphosphine (P(*t*-Bu)$_3$) (0.03 M in toluene, 1 mL, 0.03 mmol) and 1-bromo-4-iodobenzene (390 mg, 1.3 mmol). The resulting mixture was refluxed for 8 h under nitrogen atmosphere. Then the reaction mixture was let to cool down to room temperature and quenched with saturated aqueous $NaHCO_3$ (20 mL). The

organic layer was separated and the aqueous layer was extracted with dichloromethane (DCM) (3 × 25 mL). The combined organic layers were washed with water, dried over anhydrous $MgSO_4$, and then concentrated under vacuum to give the crude product **1**, which was purified by column chromatography on silica gel (PE/DCM, 5:1) to afford the pure compound **1** as a white solid (192 mg, 50%). ^{1}H NMR (400 MHz, $CDCl_3$, TMS), δ(ppm): 7.82 (d, *J* = 7.6 Hz, 1H), 7.53 (d, *J* = 7.2 Hz, 1H), 7.49–7.34 (m, 5H), 7.28 (d, *J* = 12.5 Hz, 1H), 7.08 (d, *J* = 8.4 Hz, 2H), 6.25 (d, *J* = 8.4 Hz, 2H), 6.04 (s, 1H), 3.80 (s, 3H). ^{13}CNMR (100 MHz, $CDCl_3$) δ: 156.15, 147.56, 142.80, 141.12, 135.90, 134.25, 131.26, 130.92, 130.17, 129.64, 129.61, 128.49, 127.70, 127.36, 127.18, 113.48, 109.77, 102.19, 55.42.

10-methoxy-5-(4-(thiophen-2-yl)phenyl)-5*H*-dibenzo[*b,f*]azepine (2)

To a mixture of **1** (500 mg, 1.33 mmol) and 2-(tributyltin)thiophene (740 mg, 2.0 mmol) in toluene (25 mL) was added $Pd(PPh_3)_4$ (57 mg, 0.05 mmol) and then refluxed for 12 h under nitrogen atmosphere. After cooled down to room temperature (RT) and quenched with water, the mixture was extracted with DCM (3 × 30 mL). The combine organic layers were washed with water and dried with anhydrous $MgSO_4$. After filtration, the solvent was removed under vacuum and the residue was purified by silica gel column chromatography with (PE/DCM, 6/1) as eluent to obtain **2** as a white solid (100 mg, 19%). ^{1}H NMR (400 MHz, $CDCl_3$, TMS), δ(ppm): 7.82 (d, *J* = 5.6 Hz, 1H), 7.66–7.19 (m, 9H), 7.18–6.91 (m, 3H), 6.41 (d, *J* = 5.9 Hz, 2H), 6.06 (s, 1H), 3.80 (s, 3H). ^{13}CNMR (100 MHz, $CDCl_3$) δ: 156.30, 148.06, 145.18, 143.10, 136.10, 134.49, 130.90, 130.22, 129.78, 129.74, 128.53, 127.91, 127.69, 127.31,

127.16, 126.62, 124.61, 123.00, 112.16, 102.41, 68.10, 55.43.

10-methoxy-5-(4-(5-(trimethylstannyl)thiophen-2-yl)phenyl)-5H-dibenzo[b,f]azepine (3)

2.5 M *n*-BuLi (0.3 mL, 0.75 mmol) was added dropwise to a solution of **2** (98 mg, 0.26 mmol) in dry THF (15 mL) at –78 °C under nitrogen. After stirring for 2 h, trimethylchlorotin (0.5 mL, 1.9 mmol) was added. The reaction mixture was stirred for additional 30 min and then gradually warmed to RT and stirred for 12 h. The reaction was quenched with water (30 mL) and the resulting mixture was extracted with DCM (3 × 25 mL). The organic layers were combined and washed with water and dried over anhydrous $MgSO_4$. After filtration, the solvent was removed under vacuum to give product **3** (60 mg, 32%). ^{1}H NMR (400 MHz, $CDCl_3$, TMS), δ(ppm): 7.81 (d, *J* = 7.8 Hz, 1H), 7.50 (dd, *J* = 21.9, 3H), 7.39 (d, *J* = 13.7 Hz, 5H), 7.17 (s, 1H), 7.07 (t, *J* = 19.0 Hz, 2H), 6.40 (d, *J* = 8.6 Hz, 2H), 6.06 (s, 1H), 3.79 (s, 3H), 0.46-0.20 (m, 9H).

4-(thiophen-2-yl)aniline (4)

$Pd(PPh_3)_4$ (134 mg, 0.116 mmol) was added to a solution of 4-bromoanilines (2 g, 11.6 mmol) and 2-(tributyltin)thiophene (8.5 g, 22.7 mmol) in 50 mL toluene and the mixture was heated at 110°C for 12 h under nitrogen atmosphere. After cooling to RT, the mixture was poured into water (50 mL) and the organic layer separated. The aqueous layer was extracted with DCM (3 × 25 mL). The combined organic layers were washed with water and dried over anhydrous $MgSO_4$. The volatiles were removed under vacuum to give crude product **4**, which was purified by column

chromatography on silica gel with (PE/DCM, 4/1) as eluent to obtain **4** as a light yellow solid (1.8 g, 89%). ^{1}H NMR (400 MHz, $CDCl_3$, TMS), δ(ppm): 7.42 (d, *J* = 6.6 Hz, 2H), 7.15 (s, 2H), 7.02 (s, 1H), 6.69 (d, *J* = 6.7 Hz, 2H), 3.73 (s, 2H).

4-(10-methoxy-5H-dibenzo[b,f]azepin-5-yl)-N-(4-(10-methoxy-5H-dibenzo[b,f]azepin-5-yl)phenyl)-N-(4-(thiophen-2-yl)phenyl)aniline (5)

To a solution of compound **4** (0.35 g, 2 mmol), t-BuONa (1 g, 8.0 mmol) and $Pd_2(dba)_3$ (110 mg, 0.12 mmol) in dry toluene (50 mL) was added P(t-Bu)$_3$ (1 M in toluene, 0.3 mL) and **1** (2.26 g, 6.0 mmol). The resulting mixture was refluxed for 8 h in nitrogen atmosphere. After cooling down to RT, the reaction mixture was quenched with saturated aqueous $NaHCO_3$ (20 mL). The organic layer was separated and the aqueous layer was extracted with DCM (3 × 35 mL). The combine organic layers were washed with water and dried over anhydrous $MgSO_4$. The volatiles were removed under vacuum to give the crude product **5**, which was purified by column chromatography on silica gel with (PE/DCM, 5/1) as eluent to obtain **5** as a light yellow solid (1.35 g, 87%). 1HNMR (400 MHz, $CDCl_3$, TMS), δ(ppm): 7.66 (d, J = 5.5 Hz, 2H), 7.51 (s, 2H), 7.47 – 7.20 (m, 13H), 7.13 (s, 2H), 6.95 (s, 2H), 6.68 (d, J = 5.5 Hz, 4H), 6.50 (d, J = 5.1 Hz, 2H), 6.27 – 5.96 (m, 6H), 3.69 (s, 6H). ^{13}CNMR (100 MHz, DMSO) δ: 155.83, 148.70, 145.06, 144.39, 142.96, 141.24, 137.57, 136.07, 134.35, 131.43, 130.63, 130.09, 129.75, 128.66, 128.49, 128.08, 127.62, 127.42, 127.16, 126.55, 124.70, 124.13, 121.93, 118.08, 112.48, 102.96, 55.79. MALDI-MS calcd for $C_{53}H_{40}N_2O_2S$ [M]+, 769.281; found, 769.441.

4-(10-methoxy-5H-dibenzo[b,f]azepin-5-yl)-N-(4-(10-methoxy-5H-dibenzo[b,f]azepin-5-yl)phenyl)-N-(4-(5-(trimethylstannyl)thiophen-2-yl)phenyl)aniline (6)

2.5 M n-BuLi (0.3 mL, 0.75 mmol) was added dropwise to a solution of compound **5** (551 mg, 1 mmol) in dry THF (15 mL) at –78 ^{o}C under nitrogen. After stirring for 1 h at –78 ^{o}C, trimethyl tin (0.47 mL, 1.7 mmol) was added. The reaction mixture was stirred at –78 °C for additional 30 min and then gradually warmed to room temperature and further stirred for 12 h. Then the reaction was quenched by adding water (30 mL) and the resulting mixture was extracted with DCM (3 × 25 mL). The organic layers were combined, washed with water and dried over anhydrous $MgSO_4$. The volatiles were removed under vacuum to give compound **6** as a yellow oil (320 mg) in 45%. ^{1}HNMR (400 MHz, $CDCl_3$, TMS), δ(ppm): 7.77 (s, 2H), 7.47 (br, 6H), 7.34 (br, 8H), 7.08 (s, 2H), 6.77 (br, 6H), 6.29 (br, 4H), 6.06 (br, 2H), 3.78 (d, *J* = 25.4 Hz, 6H), 0.51-0.20 (m, 9H).

Synthesis of **8**

A mixture of compound of **7** (1.28 g, 2 mmol), $Pd_2(dba)_3$ (73 mg, 0.08 mmol), P(*o*-tyl)$_3$ (50 mg, 0.16 mmol), and Na_2CO_3 (2.76 g, 20 mmol) in 60 mL of THF was heated to 50 °C. After stirring for 30 min, a solution of 5-formylthiophen-2-yl boronic acid (0.31 g, 2 mmol) in THF (10 mL) was injected to the mixture. The mixture was then heated at 80 °C for 10 h. After cooling to RT and quenched with water, the resulting solution was extracted with DCM (3 × 30 mL). The combined organic layers were washed with water and dried over anhydrous $MgSO_4$. The volatiles were removed under vacuum and the residue was purified by column chromatography

silica gel with PE/DCM (V/V, 5/2) as eluent to obtain **8** as a purple solid (750 mg, 55%). ^{1}HNMR (400 MHz, $CDCl_3$, TMS), δ(ppm): 9.96 (s, 1H), 9.23 (d, *J* = 8.3 Hz, 1H), 9.08 (d, *J* = 8.6 Hz, 1H), 7.77 (s, 1H), 7.50 (s, 1H), 7.37 (d, *J* = 9.2 Hz, 1H), 7.16 (d, *J* = 14.7 Hz, 1H), 7.04 (s, 1H), 6.92 (s, 1H), 3.69 (dd, *J* = 31.1, 9.4 Hz, 4H), 1.86 (s, 2H), 1.33 (dd, *J* = 29.4, 18.9 Hz, 16H), 1.08-0.70 (m, 12H).

Synthesis of **9**

Compound **3** (150 mg, 0.275 mmol), compound **8** (200 mg, 0.3 mmol), $Pd(PPh_3)_4$ (13 mg, 0.011 mmol) and 15 mL toluene were mixed together in a 25 mL flask and the mixture was heated at 110 °C for 12 h. The mixture was then cooled down to room temperature and extracted with DCM (3×10 mL). The combined organic layers were washed with water and dried over anhydrous $MgSO_4$. The volatiles were removed under vacuum and the residue was purified by column chromatography on silica gel with PE/EA (V/V, 7/1) as eluent to obtain **9** as a black solid (120 mg, 44%). ^{1}HNMR (400 MHz, $CDCl_3$, TMS), δ(ppm): 9.92 (s, 1H), 9.17 (dd, *J* = 23.9, 8.4 Hz, 2H), 7.84 (d, *J* = 7.9 Hz, 1H), 7.76 (d, *J* = 3.6 Hz, 1H), 7.61 – 7.30 (m, 15H), 7.10 (d, *J* = 3.3 Hz, 1H), 7.03 (s, 1H), 6.95 (s, 1H), 6.44 (d, *J* = 8.6 Hz, 2H), 6.07 (s, 1H), 3.81 (s, 3H), 3.71 (d, *J* = 15.6 Hz, 4H), 1.88 (s, 2H), 1.47-1.04 (m, 16H), 1.03-0.59 (m, 12H). ^{13}CNMR (100 MHz, $CDCl_3$) δ: 182.38, 168.39, 155.94, 153.58, 148.44, 146.16, 145.71, 145.21, 141.29, 140.57, 138.36, 134.32, 133.34, 130.49, 130.13, 129.51, 128.46, 127.64, 126.37, 123.91, 122.93, 122.23, 122.21, 120.22, 119.50, 118.51, 118.07, 112.14, 105.30, 104.42, 102.14, 55.42, 44.13, 37.80, 30.86, 28.86, 23.09, 14.13, 14.09, 10.84. MALDI-MS calcd for $C_{62}H_{63}N_3O_4S_2$ $[M]^+$, 976.426; found,

976.549.

Synthesis of **10**

Compound **6** (160 mg, 0.208 mmol), compound **8** (162 mg, 0.25 mmol), $Pd(PPh_3)_4$ (12 mg, 0.01 mmol) and 15 mL toluene were mixed together in a 25 mL flask and the mixture was heated at 110 °C for 12 h. The mixture was then cooled down to room temperature and extracted with DCM (3×10 mL). The combined organic layers were washed with water and dried over anhydrous $MgSO_4$. The volatiles were removed under vacuum and the residue was purified by column chromatography on silica gel with PE/EA (V/V, 7/1) as eluent to obtain **10** as a black solid (110 mg, 38%). ^{1}H NMR (400 MHz, $CDCl_3$) δ(ppm): 9.91 (s, 1H), 9.20 (d, *J* = 8.4 Hz, 1H), 9.14 (d, *J* = 8.2 Hz, 1H), 7.77 (br, 4H), 7.72 (s, 2H), 7.63–7.29 (m, 24H), 6.84 (dd, *J* = 120.7, 49.3 Hz, 9H), 6.32 (s, 5H), 6.07 (s, 2H), 3.82 (s, 6H), 3.73 (s, 4H), 1.35 (dd, *J* = 41.3, 20.1 Hz, 18H), 1.03–0.73 (m, 12H). ^{13}CNMR (100 MHz, CDCl3) δ: 182.69, 168.63, 168.43, 156.23, 153.61, 149.35, 149.22, 149.12, 146.47, 146.05, 145.54, 145.17, 143.45, 142.93, 141.72, 140.96, 138.60, 137.66, 136.05, 135.62, 134.47, 133.38, 130.69, 130.48, 130.05, 129.79, 129.71, 128.32, 127.52, 127.00, 126.85, 126.58, 126.20, 124.80, 124.28, 122.98, 120.46, 118.46, 112.58, 104.44, 102.59, 55.43, 43.95, 37.81, 30.86, 28.88, 28.83, 24.31, 23.09, 14.15, 14.10, 10.86, 10.84.MALDI-MS calcd for $C_{89}H_{83}N_5O_5S_2$ [M]+, 1364.584; found, 1364.832.

Synthesis of **YC-1**

Compound **9** (200 mg, 0.19 mmol), 2-cyanoacetic acid (200 mg, 2.2 mmol), ammonium acetate (320 mg) in acetic acid (30 mL) were heated to 120 °C under

nitrogen atmosphere for 24 h. After cooling down to room temperature, the mixture was poured into water. The precipitate was filtered off and purified by column chromatography on silica gel using DCM/CH_3OH (15/1,V/V) as eluent to provide **YC-1** as a dark solid (80 mg, 38%).^{1}HNMR (400 MHz, DMSO-d6, TMS), δ(ppm): 9.14–8.90 (m, 2H), 8.21 (s, 1H), 8.05 (s, 1H), 7.76 (d, J = 7.4 Hz, 2H), 7.62 (d, J = 24.3 Hz, 4H), 7.54–7.22 (m, 8H), 7.16 (d, J = 8.8 Hz, 2H), 7.05 (s, 1H), 6.93 (s, 1H), 6.27 (d, J = 7.9 Hz, 1H), 6.19 (s, 1H), 3.75 (s, 3H), 3.62 (s, 4H), 1.76 (s, 2H), 1.10–1.31 (m, 20H), 0.85 (d, J = 23.8 Hz, 8H). MALDI-MS calcd for $C_{65}H_{64}N_6O_5S_2$ $[M]^+$, 1044.432; found, 1044.519.

Synthesis of **YC-2**

Compound **10** (150 mg, 0.11 mmol), 2-cyanoacetic acid (183 mg, 2.0 mmol), ammonium acetate (290 mg) in acetic acid (25 mL) were heated to 120 °C under nitrogen atmosphere for 24 h. After cooling to room temperature, the mixture was poured into water. The precipitate was filtered off and purified by column chromatography on silica gel using DCM/CH_3OH (15/1,V/V) as eluent to provide **YC-2** as a dark solid (63 mg, 40%). ^{1}HNMR (400 MHz, DMSO-d6, TMS), δ (ppm): 8.99 (s, 2H), 8.23 (s, 1H), 8.09 (s, 1H), 7.70 (dd, J = 22.6, 7.4 Hz, 2H), 7.53 (s, 1H), 7.48 – 7.18 (m, 14H), 7.14 (s, 1H), 6.98 (s, 1H), 6.88 (s, 1H), 6.69 (d, J = 7.1 Hz, 4H), 6.55 (d, J = 7.0 Hz, 1H), 6.27–6.09 (m, 5H), 3.72 (s, 6H), 3.60 (s, 4H), 1.75 (s, 2H), 1.19 (d, J = 75.3 Hz, 20H), 0.96–0.63 (m, 8H). MALDI-MS calcd for $C_{92}H_{84}N_6O_6S_2$ $[M]^+$, 1431.589; found, 1431.755.

3. Results and discussion

3.1. Synthesis and characterized

The synthetic routes of the two dyes **YC-1** and **YC-2** are described in **Scheme 1**. Intermediates **1** and **5** were prepared by the Buchwald-Hartwig amination via the palladium-catalyzed cross-coupling of amines (10-Methoxy iminostilbene or **4**) with aryl halides (4-bromoiodobenzene or **1**). Typical Stille coupling reactions between aryl bromide (**1** and 4-bromoaniline) and tributyl(thiophen-2-yl)stannane were carried out to afford compound **2** in moderate yield (19%) and compound **4** in high yield (89%). Intermediates **2** and **5** were reacted with $Sn(CH_3)_3Cl$ to give compound **3** and **6** in yield of 32% and 45%, respectively. Compound **8** was obtained via Suzuki coupling reaction between intermediate **7** and 5-formylthiophen-2-ylboronic acid in a yield of 55%. The key aldehyde precursors of **9** and **10** were synthesized through Stille coupling of **3** (or **6**) and **8** in 44% and 38% yields, respectively. Finally, Knoevenagel condensation of these aldehydes with cyanoacetic acid gave the dyes **YC-1** and **YC-2**. Both target dyes were characterised by ^{1}H NMR and TOF-Mass.

3.2. Photophysical properties

The UV-vis absorption spectra of **YC-1** and **YC-2** are shown in **Figure 1** and the corresponding data are listed in **Table 1**. Panchromatic absorption with two typical bands is observed for **YC-1** and **YC-2** both in solution and on neat film. The absorption band between 340 nm and 470 nm with the maximum extinction coefficient (ε) of ≈ 3-5 × 10^4 M^{-1} cm^{-1} is attributed to the localized aromatic π–π* transitions, while the band at 470–800 nm (ε ≈ 2-4 × 10^4 M^{-1} cm^{-1}) is ascribed to the

intramolecular charge transfer transition (ICT) [41]. **YC-2** exhibits a 31 nm red shift of the absorption band at long-wavelength both in solution and neat film compared to **YC-1**, ascribed to the larger donor group in **YC-2**. Additionally, **YC-2** displays a lower ε at long-wavelength than **YC-1** pointing to a lower oscillator strength for the ICT transition. Compared to the absorption in solution, a similar absorption bands with slight hypochromic shift (*ca.* 18 nm) are observed in neat film. This result can be presumably explained by the formation of H-type aggregates [41].

When both the dyes were adsorbed onto 2.0 μm thick TiO_2 films, similar absorption bands with remarkable blue shift are observed (23 nm for **YC-1** and 40 nm for **YC-2**) compared to that achieved in solution (**Figure 2** and **Table 1**). According to previous reports, this blue shift is caused by the deprotonation of the dyes on TiO_2 film and formation of H-aggregates [41,42].

3.3. Electrochemical property

To investigate the possibility of electron transfer from the dyes to TiO_2, cyclic voltammetry was carried out to estimate the redox potentials of **YC-1** and **YC-2** and the data are summarized in **Table 1**. The oxidation potentials of **YC-1** and **YC-2** are located at 0.81 V and 0.72 V (Fc/Fc^+ is 0.46 V *vs* Ag/AgCl, Fc/Fc^+ is 0.63 V *vs* NHE [43]) versus Ag/AgCl electrode, respectively (**Figure 3**). Both the values of oxidation potential (**YC-1**: 0.98 V *vs* NHE, **YC-2**: 0.89 V *vs* NHE) are higher than that of iodide/triiodide (0.35 V *vs* NHE) [18,42], indicating **YC-1** and **YC-2** can provide ample driving force for the dye regeneration. Compared to **YC-1**, the additional 10-Methoxy iminostilbene and triphenylamine units in **YC-2** decrease its oxidation

potential by 90 mV owing to increased donor ability. On the other hand, the zero-zero transition energies ($E_{0\text{-}0}$) are estimated to be 1.67 V (**YC-1**) and 1.56 V (**YC-2**) based on the absorption thresholds. Estimated from oxidation potentials and $E_{0\text{-}0}$, the optical reduction potentials of both dyes are determined to be –0.69 V and –0.67 V (*vs* NHE) for **YC-1** and **YC-2**, respectively. Both dyes show almost the same reduction potentials due to the same acceptor units. The optical reduction potentials lie above the conduction band of TiO_2 (–0.5 V *vs* NHE) [44], favoring the injection of electrons from the dyes to the TiO_2.

3.4. Theoretical calculations

In order to investigate the relationship between electronic distribution and molecular structure, density functional theory (DFT) calculations were performed to optimize the geometry of both dyes based on Gaussian 09 at B3LYP/6-31G(d) level. As shown in **Figure 4**, a similar pattern of highest occupied molecular orbitals (HOMOs) are observed at thiophene and 5-phenyl-5H-dibenzo[*b*,*f*]azepine units for **YC-1** and **YC-2**. Conversely, the lowest unoccupied molecular orbitals (LUMOs) display a different electron population. For **YC-1**, the LUMO is delocalized across the anchoring group, isoindigo, thiophene and 5-phenyl-5H-dibenzo[*b*,*f*]azepine moieties, while the LUMO of **YC-2** is only located at anchoring group. This larger HOMO-LUMO overlap in **YC-1** points to a more effective intermolecular charge transfer in **YC-1** compared to **YC-2**.

3.5. Photovoltaic performance

The performance of **YC-1** and **YC-2** as sensitizer for dye-sensitized solar cells

were evaluated at 100 mW cm^{-2} under simulated AM1.5G solar light. The current-density-voltage (*J-V*) curves of the devices are shown in **Figure 5** and the performance parameters are summarized in **Table 2**. The DSSCs based on **YC-1** showed a short-circuit photocurrent density (J_{sc}) of 12.12 mA cm^{-2}, an open-circuit voltage (V_{oc}) of 0.53 V, and a fill factor (FF) of 68.9%, corresponding to an overall η of 4.38%. **YC-2**-based DSSCs exhibited a J_{sc} of 4.84 mA cm^{-2}, a V_{oc} of 0.48 V, and an FF of 63.4%, achieving η of 1.46%. All the photovoltaic parameters of the **YC-1** are higher than those of **YC-2**, in particular the difference in short-circuit current is striking. The latter is mainly attributed to the large difference of IPCE between the two dyes in the 450-650 nm interval, where the intensity of incident photon flux is the highest.

To gain further insight into the influence of molecular structure on the current density of the devices, the incident photo-to-current conversion efficiency (IPCE) of the devices were measured (**Figure 6**). Both dyes show two well-separated peaks at 349 nm and 419 nm and one broad peak between 500 nm and 800 nm. The shape of the spectra is reminiscent of the absorption spectra with a blue shift as observed in the absorption spectra of the TiO_2 films. Importantly the IPCE of **YC-1** based device is about 61 %, 48 % and 31 % at 349 nm, 419 nm 559 nm, respectively while **YC-2** based device exhibits IPCE of only 51 %, 38 % and 15 % at the same wavelengths. Therefore the IPCE of the **YC-1** based device is about 10 % higher across the whole visible wavelength range than that of **YC-2** based device. This result is ascribed to the better light harvesting properties of **YC-1** (higher epsilon) than **YC-2**, which was

expected from the absorption spectra (**Figure 1**). Consequently, the higher IPCE values of **YC-1** results in the much higher J_{sc} compared to **YC-2**.

3.6. Electrochemical Impedance Spectroscopy (EIS)

Electrochemical impedance spectroscopy (EIS) was carried out to explore the electron recombination dynamics in the devices. The Nyquist plots and bode plots of DSSCs based on **YC-1** and **YC-2** were recorded in dark with applied bias of 0.55 V and the results are shown in Figure **7** and Figure **8**.

Estimated from the fitting of the EIS spectra with an electrochemical model [38,45], the series resistances (R_S), charge transfer resistances at the Pt/electrolyte interface (R_{CE}) and dye/TiO_2/electrolyte interface (R_{rec}) were calculated (**Table 3**). The R_S and R_{CE} corresponding to the arc in high frequency region (**Figure 4 inset**) show almost the same value in both DSSCs owing to the same electrode and electrolyte. R_{rec} corresponds to the middle arc in low frequency region and indicates that the R_{rec} of **YC-1** based device is distinctly higher than that of **YC-2** based device.

The intermediate frequency peak in the EIS Bode plots is assigned to the recombination at the TiO_2/electrolyte interface. As seen from **Figure 8**, the intermediate frequency peak of **YC-1** based device shows a lower frequency than that of **YC-2** based device. Based on this result [46], the electron lifetimes (τ_e, $1/(2\pi f)$) are assessed to be 12.5 ms and 7.2 ms for **YC-1** and **YC-2**, respectively. **YC-1** possesses a longer τ_e in titania films, which could be attributed to a lower rate of charge recombination and higher V_{oc}. Additionally, the radius of the intermediate arc in **Figure 8** describes the charge transfer impedance at the TiO_2/electrolyte interface [42].

YC-1 shows a larger arc than **YC-2**, implying that **YC-1** has a more difficult charge transfer than YC-2, which results in a higher electron density in the titania film leading to superior performance for its corresponding device. Likewise, this result could be derived from Nyquist plot (**Figure 7**).

4. Conclusions

In conclusion, two D-π-A-π-A dyes based on 5-phenyl-5*H*-dibenzo[*b*,*f*]azepine donor group were synthesized and characterized. Compared to the reported dyes **ID1**, which uses a triphenylamine donor group, **YC-1** and **YC-2** showed red-shifted absorption and enhancement of molar extinction coefficient due to extended conjugation. **YC-2** possesses stronger donor ability as shown by the decreased oxidation potential compared to **YC-1**. The influence of the different donor groups on the photovoltaic performance of sensitized cells was explored. **YC-1** exhibited the best power conversion efficiency of 4.38% (J_{sc} = 12.12 mA cm^{-2}, V_{oc} = 0.53 V and FF = 68.89) for the DSSCs without any co-sensitizer, which is almost three folds the efficiency of **YC-2**. This result is attributed to the more effective ICT and longer lifetime of electron injected in the titania of **YC-1** as evidenced by DFT and EIS, leading to an improvement of photocurrent and open circuit voltage, and, thus power conversion efficiency. This research illustrated: (1) 5-phenyl-5*H*-dibenzo[*b*,*f*]azepine could be a promising donor moiety in DSSCs dyes; (2) The balance between spatial structure and intermolecular charge transfer plays a key role for the high efficiency in sensitizer. Future work will be focus on optimized DSSCs with the co-sensitizer and

cobalt electrolyte to further improve the performance.

Acknowledgements

Financial support from the National Natural Science Foundation of China (21202139, 51473140, 51273168 and 21172073), the Program for Innovative Research Cultivation Team in University of Ministry of Education of China (1337304), the Innovation Group in Hunan Natural Science Foundation (12JJ7002),. The Scientific Research Fund of Hunan Provincial Education Department (12B123, 10C1294), Natural Science Foundation of Hunan (12JJ4019, 11JJ3061). The Open Fund of the State Key Laboratory of Luminescent Materials and Devices (South China University of Technology) (2015-skllmd-08).

References

[1] Graetzel M, Janssen RA, Mitzi DB, Sargent EH. Materials Interface Engineering for Solution-Processed Photovoltaics. Nature 2012;488:304-12.

[2] O'regan B, Grätzel M. A Low-Cost, High-Efficiency Solar Cell Based on Dye-Sensitized Colloidal TiO_2 Films. Nature 1991;353:737-40.

[3] Wang CL, Shiu JW, Hsiao YN, Chao PS, Wei-Guang Diau E, Lin CY. Co-Sensitization of Zinc and Free-Base Porphyrins with an Organic Dye for Efficient Dye-Sensitized Solar Cells. J Phys Chem C 2014;118:27801-7.

[4] Hardin BE, Snaith HJ, McGehee MD. The Renaissance of Dye-Sensitized Solar Cells. Nat Photonics 2012;6:162-9.

[5] Li LL, Diau EWG. Porphyrin-Sensitized Solar Cells. Chem Soc Rev 2013;42:291-304.

[6] Stangel C, Bagaki A, Angaridis PA, Charalambidis G, Sharma GD, Coutsolelos AG. “Spider”-Shaped Porphyrins with Conjugated Pyridyl Anchoring Groups as Efficient Sensitizers for Dye-Sensitized Solar Cells. Inorg Chem 2014;53:11871-81.

[7] Mukherjee S, Bowman DN, Jakubikova E. Cyclometalated Fe (II) Complexes as Sensitizers in Dye-Sensitized Solar Cells. Inorg Chem 2014;54:560-9.

[8] Yella A, Lee HW, Tsao HN, Yi C, Chandiran AK, Nazeeruddin MK, Diau EWG, Yeh CY, Zakeeruddin SM, Grätzel M. Porphyrin-Sensitized Solar Cells with Cobalt (II/III)-Based Redox Electrolyte Exceed 12 Percent Efficiency. Science 2011;334:629-34.

[9] Ito S, Miura H, Uchida S, Takata M, Sumioka K, Liska P, Comte P, Péchy P, Grätzel M. High-Conversion-Efficiency Organic Dye-Sensitized Solar Cells with a Novel Indoline Dye. Chem Commun 2008;5194-6.

[10] DiáCenso D. A Structural Study of DPP-Based Sensitizers for DSC Applications. Chem Commun 2012;48:10724-6.

[11] Pei K, Wu Y, Islam A, Zhang Q, Han L, Tian H, Zhu W. Constructing High-Efficiency D-A-π-A-Featured Solar Cell Sensitizers: A Promising Building Block of 2, 3-Diphenylquinoxaline for Antiaggregation and Photostability. ACS Appl Mater Interfaces 2013;5:4986-95.

[12] Choi H, Chen YS, Stamplecoskie KG, Kamat PV. Boosting the Photovoltage of Dye-Sensitized Solar Cells with Thiolated Gold Nanoclusters. J Phys Chem Lett 2014;6: 217-23.

[13] Mathew S, Yella A, Gao P, Humphry-Baker R. Curchod BF, Ashari-Astani N, Tavernelli I, Rothlisberger U. Nazeeruddin MK. Grätzel M. Dye-Sensitized Solar Cells with 13% Efficiency Achieved through the Molecular Engineering of Porphyrin Sensitizers. Nat Chem 2014;6:242-7.

[14] Han L, Islam A, Chen H, Malapaka C, Chiranjeevi B, Zhang S, Yang X, Yanagida M. High-Efficiency Dye-Sensitized Solar Cell with a Novel Co-Adsorbent. Energy Environ Sci 2012;5:6057-60.

[15] Cao Y, Bai Y, Yu Q, Cheng Y, Liu S, Shi D, Gao F, Wang P. Dye-Sensitized Solar Cells with a High Absorptivity Ruthenium Sensitizer Featuring a 2-(Hexylthio) Thiophene Conjugated Bipyridine. J Phys Chem C 2009;113:6290-7.

[16] Chou CC, Hu FC, Yeh HH, Wu HP, Chi Y, Clifford JN, Palomares E, Liu SH, Chou PT, Lee GH. Highly Efficient Dye-Sensitized Solar Cells Based on Panchromatic Ruthenium Sensitizers with Quinolinylbipyridine Anchors. Angew Chem Int Ed 2014;53:178-83.

[17] Yu Q, Wang Y, Yi Z, Zu N, Zhang J, Zhang M, Wang P. High-Efficiency Dye-Sensitized Solar Cells: The Influence of Lithium Ions on Exciton Dissociation, Charge Recombination, and Surface States. ACS nano 2010;4:6032-8.

[18] Hagfeldt A, Boschloo G, Sun L, Kloo L, Pettersson H. Dye-Sensitized Solar Cells. Chem Rev 2010;110:6595-663.

[19] Zhou N, Prabakaran K, Lee B, Chang SH, Harutyunyan B, Guo P, Butler MR, Timalsina A, Bedzyk MJ. Ratner MA. Metal-Free Tetrathienoacene Sensitizers for High-Performance Dye-Sensitized Solar Cells. J Am Chem Soc 2015;137:4414-23.

[20] Wang Z, Wang H, Liang M, Tan Y, Cheng F, Sun Z, Xue S. Judicious Design of Indoline Chromophores for High-Efficiency Iodine-Free Dye-Sensitized Solar Cells. ACS Appl Mater Interfaces 2014;6:5768-78.

[21] Zhang M, Wang Y, Xu M, Ma W, Li R, Wang P. Design of High-Efficiency Organic Dyes for Titania Solar Cells Based on the Chromophoric Core of Cyclopentadithiophene-Benzothiadiazole. Energy Environ Sci 2013;6:2944-9.

[22] Zhu W, Wu Y, Wang S, Li W, Li X, Chen J, Wang ZS, Tian H. Organic D-A-π-A Solar Cell Sensitizers with Improved Stability and Spectral Response. Adv Funct Mater 2011;21: 756-63.

[23] Thongkasee P, Thangthong A, Janthasing N, Sudyoadsuk T, Namuangruk S, Keawin T, Jungsuttiwong S, Promarak V. Carbazole-Dendrimer-Based Donor-π-Acceptor Type Organic Dyes for Dye-Sensitized Solar Cells: Effect of the Size of the Carbazole Dendritic Donor. ACS Appl Mater Interfaces 2014;6:8212-22.

[24] Qian X, Zhu YZ, Song J, Gao XP, Zheng JY. New Donor-π-Acceptor Type Triazatruxene

Derivatives for Highly Efficient Dye-Sensitized Solar Cells. Org Lett 2013;15:6034-7.

[25] Qu S, Qin C, Islam A, Wu Y, Zhu W, Hua J, Tian H, Han L. A Novel D-A-π-A Organic Sensitizer Containing a Diketopyrrolopyrrole Unit with a Branched Alkyl Chain for Highly Efficient and Stable Dye-Sensitized Solar Cells. Chem Commun 2012;48:6972-4.

[26] Kang SH, Kang MS, Choi IT.; Hong JY, Ju MJ, Kim HK. D-π-A Structured Zn^{II}-Porphyrin Dyes with Thiophene Moiety for Highly Efficient Dye-Sensitized Solar Cells. ChemElectroChem 2014;1:637-44.

[27] Cui Y, Wu Y, Lu X, Zhang X, Zhou G, Miapeh FB, Zhu W, Wang ZS. Incorporating Benzotriazole Moiety to Construct D-A-π-A Organic Sensitizers for Solar Cells: Significant Enhancement of Open-Circuit Photovoltage with Long Alkyl Group. Chem Mater 2011;23:4394-401.

[28] Wu Y, Zhu W. Organic Sensitizers from D-π-A to D-A-π-A: Effect of the Internal Electron-Withdrawing Units on Molecular Absorption, Energy Levels and Photovoltaic Performances. Chem Soc Rev 2013;42:2039-58.

[29] Yum JH, Holcombe TW, Kim Y, Rakstys K, Moehl T, Teuscher J, Delcamp JH, Nazeeruddin MK, Grätzel M. Blue-Coloured Highly Efficient Dye-Sensitized Solar Cells by Implementing the Diketopyrrolopyrrole Chromophore. Sci Rep 2013;3.

[30] Snaith HJ, Schmidt-Mende L. Advances in Liquid-Electrolyte and Solid-State Dye-Sensitized Solar Cells. Adv Mater 2007;19:3187-200.

[31] Radivojevic I, Bazzan G, Burton-Pye BP, Ithisuphalap K, Saleh R, Durstock MF, Francesconi LC, Drain CM. Zirconium (IV) and Hafnium (IV) Porphyrin and Phthalocyanine Complexes as New Dyes for Solar Cell Devices. J Phys Chem C 2012;116:15867-77.

[32] Sharma D, Steen G, Korterik JP, García-Iglesias M, Vázquez P, Torres TS, Herek JL, Huijser A. Impact of the Anchoring Ligand on Electron Injection and Recombination Dynamics at the Interface of Novel Asymmetric Push-Pull Zinc Phthalocyanines and TiO_2. J Phys Chem C 2013;117:25397-404.

[33] Liang M, Chen J. Arylamine Organic Dyes for Dye-Sensitized Solar Cells. Chem Soc Rev 2013;42:3453-88.

[34] Wu Y, Marszalek M, Zakeeruddin SM, Zhang Q, Tian H, Grätzel M, Zhu W. High-Conversion-Efficiency Organic Dye-Sensitized Solar Cells: Molecular Engineering on D-A-π-A Featured Organic Indoline Dyes. Energy Environ Sci 2012;5:8261-72.

[35] Yang J, Ganesan P, Teuscher JL, Moehl T, Kim YJ, Yi C, Comte P, Pei K, Holcombe TW, Nazeeruddin MK. Influence of the Donor Size in D-π-A Organic Dyes for Dye-Sensitized Solar Cells. J Am Chem Soc 2014;136:5722-30.

[36] Chou HH, Chen YC, Huang HJ, Lee TH, Lin JT, Tsai C, Chen K. High-Performance Dye-Sensitized Solar Cells Based on 5, 6-Bis-Hexyloxy-Benzo [2, 1, 3] Thiadiazole. J Mater Chem 2012;22:10929-38.

[37] Satoh N, Nakashima T, Yamamoto K. Metal-Assembling Dendrimers with a Triarylamine Core and Their Application to a Dye-Sensitized Solar Cell. J Am Chem Soc 2005;127;13030-8.

[38] Ying W, Guo F, Li J, Zhang Q, Wu W, Tian H, Hua J. Series of New D-A-π-A Organic Broadly Absorbing Sensitizers Containing Isoindigo Unit for Highly Efficient Dye-Sensitized Solar Cells. ACS Appl Mater Interfaces 2012;4:4215-24.

[39] Numata Y, Ashraful I, Shirai Y, Han L. Preparation of Donor-Acceptor Type Organic Dyes

Bearing Various Electron-Withdrawing Groups for Dye-Sensitized Solar Cell Application. Chem Commun 2011;47:6159-61.

[40] Mei J, Graham KR, Stalder R, Reynolds JR. Synthesis of Isoindigo-Based Oligothiophenes for Molecular Bulk Heterojunction Solar Cells. Org Let 2010;12:660-3.

[41] Wang X, Yang J, Yu H, Li F, Fan L, Sun W, Liu Y, Koh ZY, Pan J. Yim WL. A Benzothiazole-Cyclopentadithiophene Bridged D-A-π-A Sensitizer with Enhanced Light Absorption for High Efficiency Dye-Sensitized Solar Cells. Chem Commun 2014;50:3965-8.

[42] Kang X, Zhang J, O'Neil D, Rojas AJ, Chen W, Szymanski P, Marder SR, El-Sayed MA. Effect of Molecular Structure Perturbations on the Performance of the D-A-π-A Dye Sensitized Solar Cells. Chem Mater 2014;26:4486-93.

[43] Li SG, Jiang KJ, Huang JH, Yang LM, Song YL. Molecular Engineering of Panchromatic Isoindigo Sensitizers for Dye-Sensitized Solar Cell Applications. Chem Commun 2014;50:4309-11.

[44] Wang Y, Chen B, Wu W, Li X, Zhu W, Tian H, Xie Y. Efficient Solar Cells Sensitized by Porphyrins with an Extended Conjugation Framework and a Carbazole Donor: From Molecular Design to Cosensitization. Angew Chem Int Ed 2014;53:10779-83.

[45] Fabregat-Santiago F, Garcia-Belmonte G, Mora-Seró I, Bisquert J. Characterization of Nanostructured Hybrid and Organic Solar Cells by Impedance Spectroscopy. Phys Chem Chem Phys 2011;13:9083-118.

[46] Lin LY, Tsai CH, Wong KT, Huang TW, Hsieh L, Liu SH, Lin HW, Wu CC, Chou SH, Chen SH. Organic Dyes Containing Coplanar Diphenyl-Substituted Dithienosilole Core for Efficient Dye-Sensitized Solar Cells. J Org Chem 2010;75:4778-85.

Tables Captions

Table 1 Photophysical data of **YC-1** and **YC-2**

Table 2 Photovoltaic performance parameters of sensitized cells

Table 3 Parameters evaluated from fitting the EIS spectra of **YC-1** and **YC-2** based DSSCs

Table 1

Dye	Absorption/nm(10^5 $M^{-1}cm^{-1}$)			$^{a}E_g^{opt}$/eV	$^{b}E^{ox}$/V	$^{c}E^{red\text{-}opt}$/V
	Solution	Neat film	On TiO_2			
YC-1	415 (0.45), 585 (0.45)	410, 563	402, 562	1.67	0.98	-0.69
YC-2	392 (0.48), 616 (0.35)	391, 600	414, 576	1.56	0.89	-0.67

[a] estimated from the edge-absorption spectra; [b] calculated from onset oxidation peaks. E_{dyes}^{ox}-$E_{FC/FC+}$+0.63 V; [c] calculated from the formulation: $E^{red\text{-}opt} = E^{g}$-$E^{ox}$

Table 2

Dye	J_{sc}/mA cm^{-2}	V_{oc}/V	FF	PCE/%
YC-1	12.12	0.53	68.89	4.38
YC-2	4.84	0.48	63.35	1.46

Table 3

Dye	R_S (Ω)	R_{CE} (Ω)	R_{rec} (Ω)	τ_e (ms)
YC-1	16.11	56.47	96.55	12.5
YC-2	16.96	41.48	63.23	7.2

Figures Captions

Chart 1 molecular structure of **ID-1**, **YC-1** and **YC-2**

Scheme 1 synthesis of **YC-1** and **YC-2**

Figure 1 UV−vis absorption spectra of **YC-1** and **YC-2** in $CHCl_3$ solution (10^{-5} M) and as neat films

Figure 2 UV−vis absorption spectra of **YC-1** and **YC-2** were measured on TiO_2 films

Figure 3 CV curves of **YC-1** and **YC-2** were measured in $CHCl_3$ solution (inset the CV curve of ferrocene)

Figure 4 Electron distributions of MOs (a: **YC-1**, b: **YC-2**)

Figure 5 *J-V* curves of **YC-1** and **YC-2** based sensitized cells

Figure 6 IPCE curves of **YC-1** and **YC-2** based sensitized cells

Figure 7 Nyquist plots of **YC-1** and **YC-2** based dye sensitized cells

Figure 8 Bode plots of **YC-1** and **YC-2** based sensitized cells

Chart 1

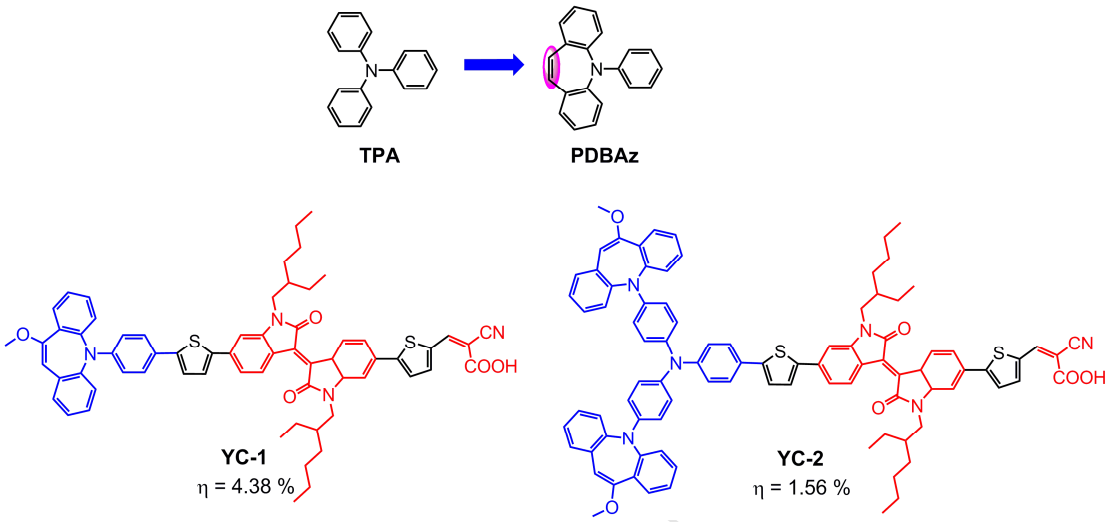

Scheme 1

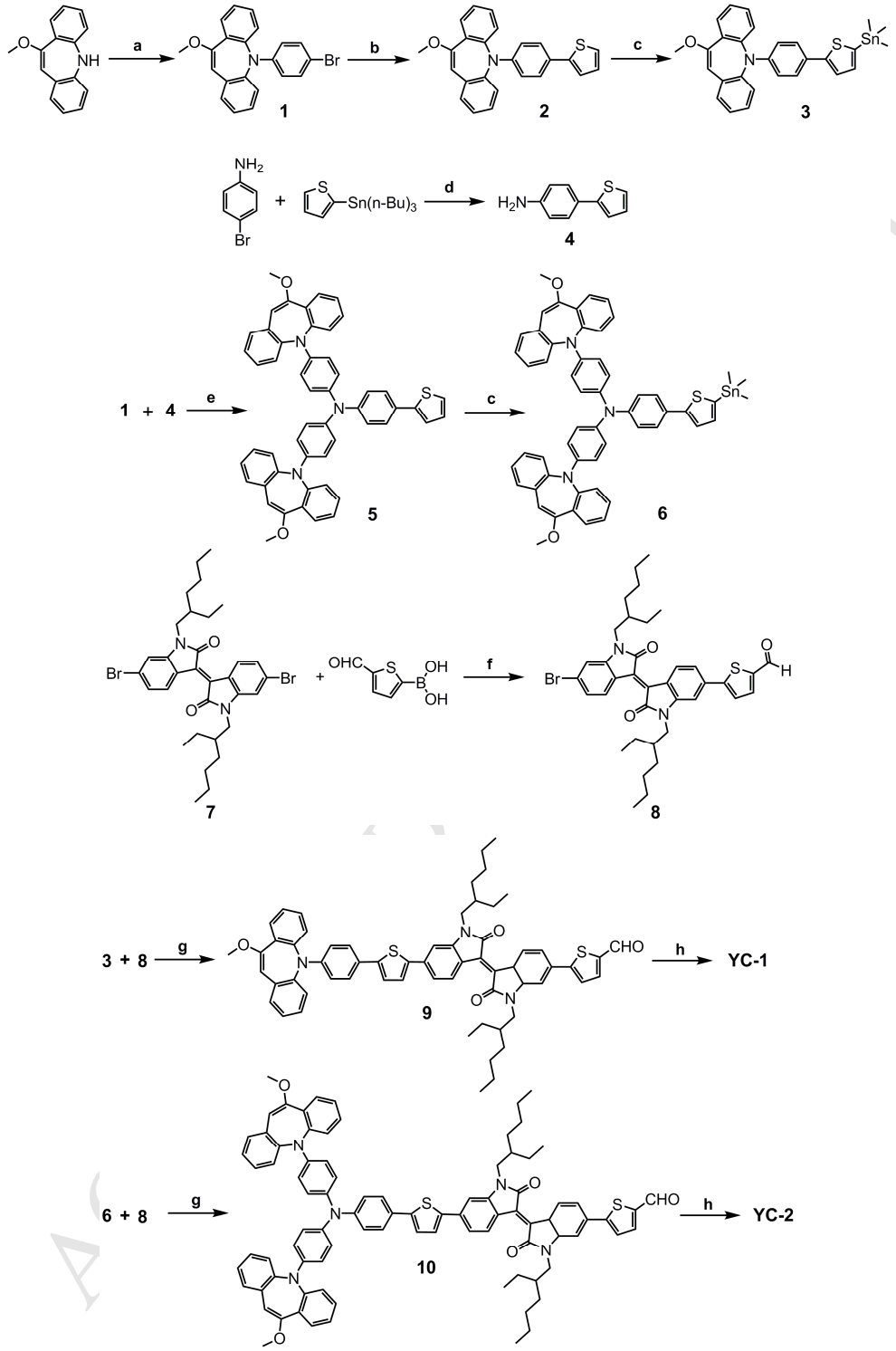

Reaction conditions: Reaction conditions: (a) 1-bromo-4-iodobenzene, $Pd_2(dba)_3$, $P(^tBu)_3$, ^{t}BuONa, toluene, reflux, overnight, 50%; (b) tributyl(thiophen-2-yl)stannane, $Pd(PPh_3)_4$, toluene, reflux, overnight, 19%; (c) $Sn(CH_3)_3Cl$, dry THF, *n*-BuLi, -78^{o}C to RT, 12 h, (**3**: 32%, **6**: 45 %); (d) $Pd(PPh_3)_4$, toluene, 110^{o}C, 12h, 89%; (e) $Pd_2(dba)_3$, $P(^tBu)_3$, ^{t}BuONa, toluene, reflux, 8h, 87%; (f) $Pd_2(dba)_3$, K_2CO_3, P(*o*-tyl)$_3$,THF, reflux, 10h, 55%; (g) $Pd(PPh_3)_4$, toluene, 110 ^{o}C, 10h (**9**: 44%, **10**: 38%); (h) CH_3COOH, CH_3COONH_4, CH_3COOCN, 120^{o}C, 24h, (**YC-1**: 38%, **YC-2**: 40%).

Figure 1

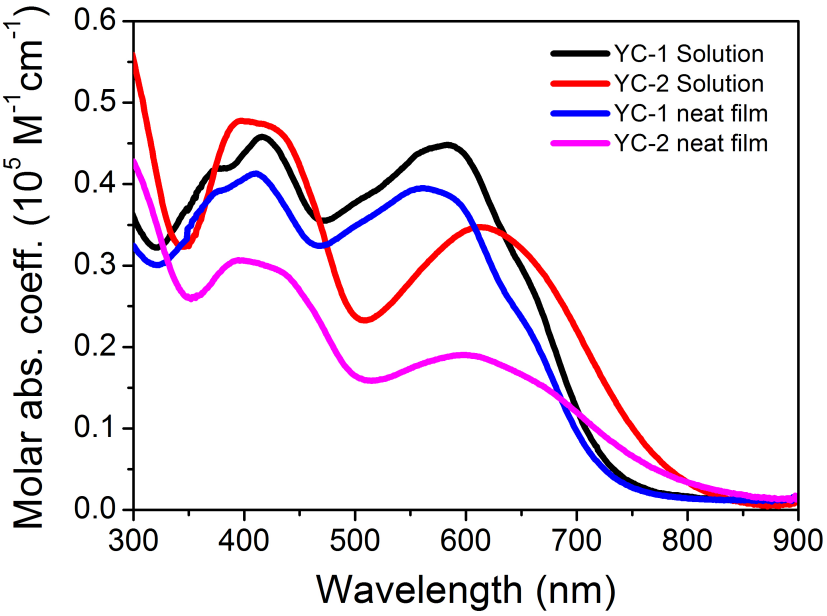

Figure 2

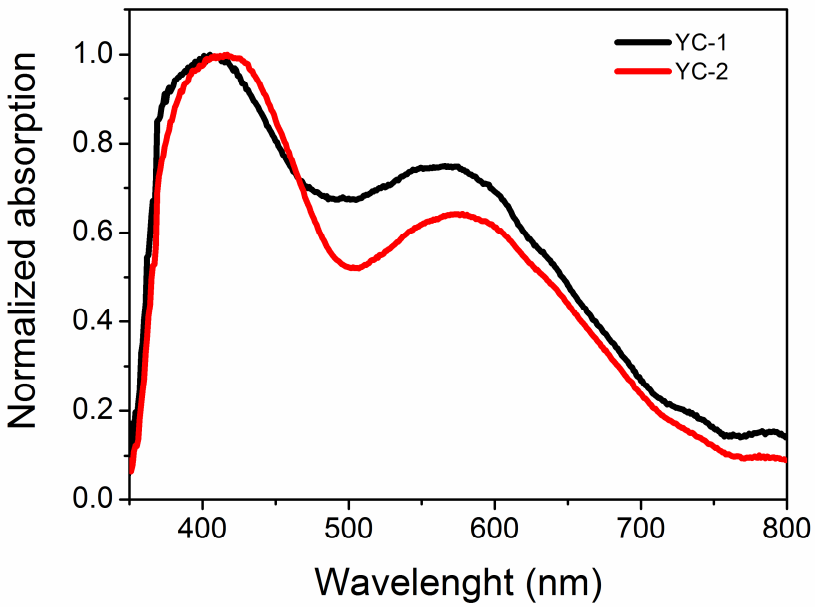

Figure 3

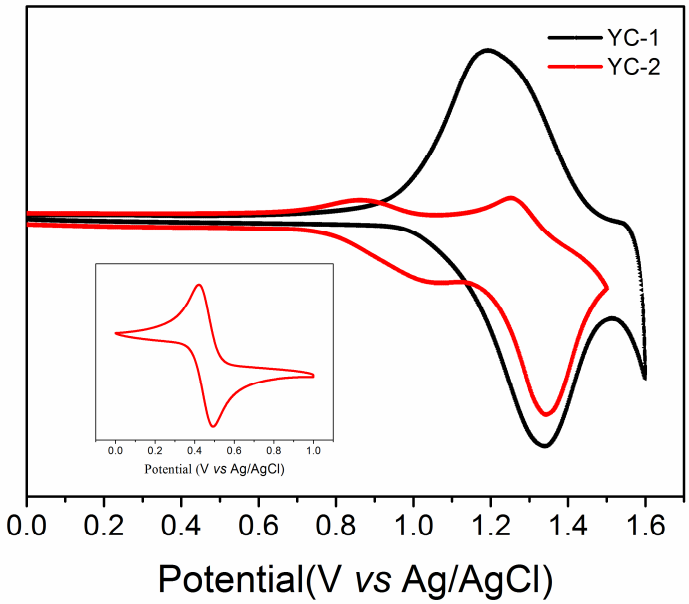

Figure 4

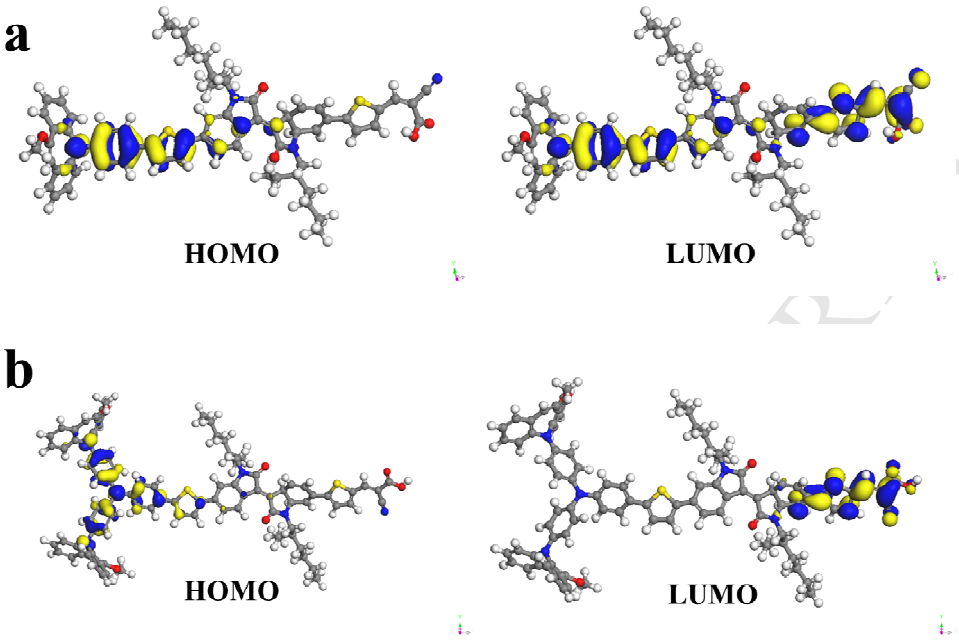

Figure 5

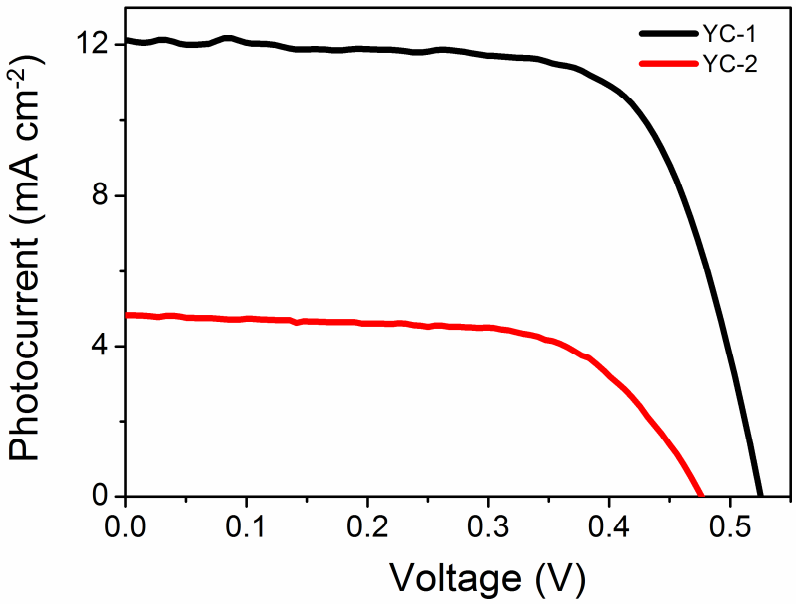

Figure 6

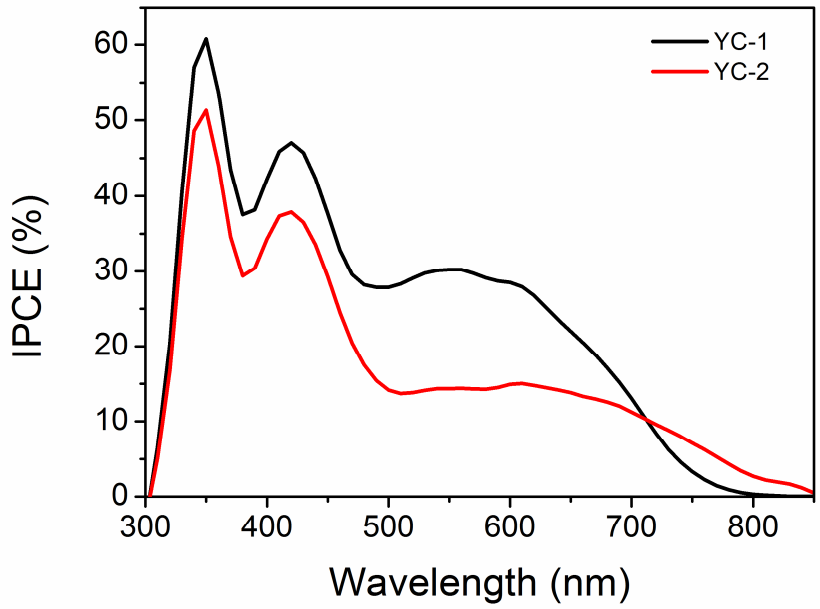

Figure 7

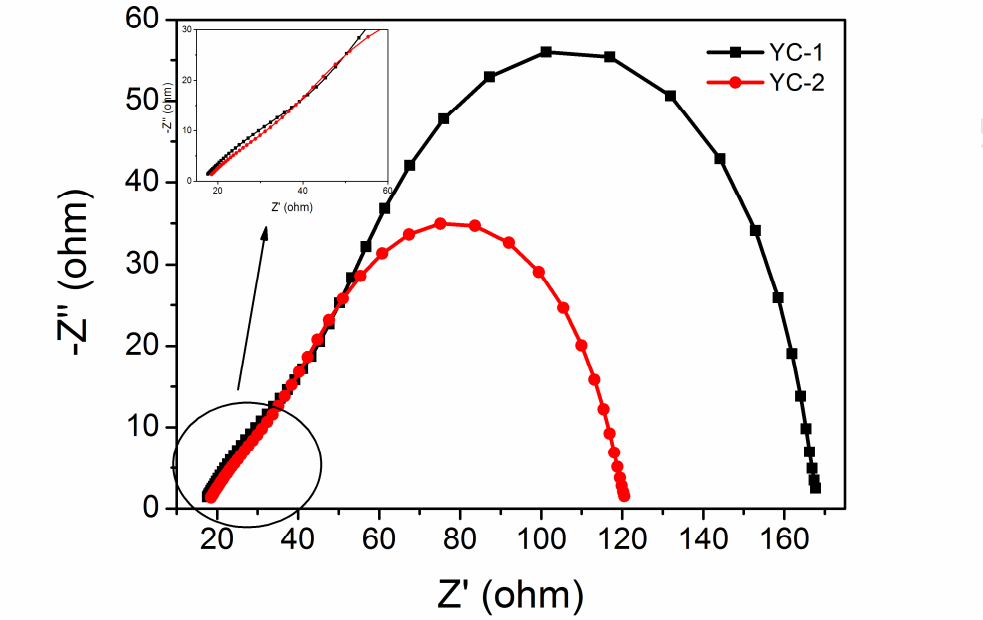

Figure 8

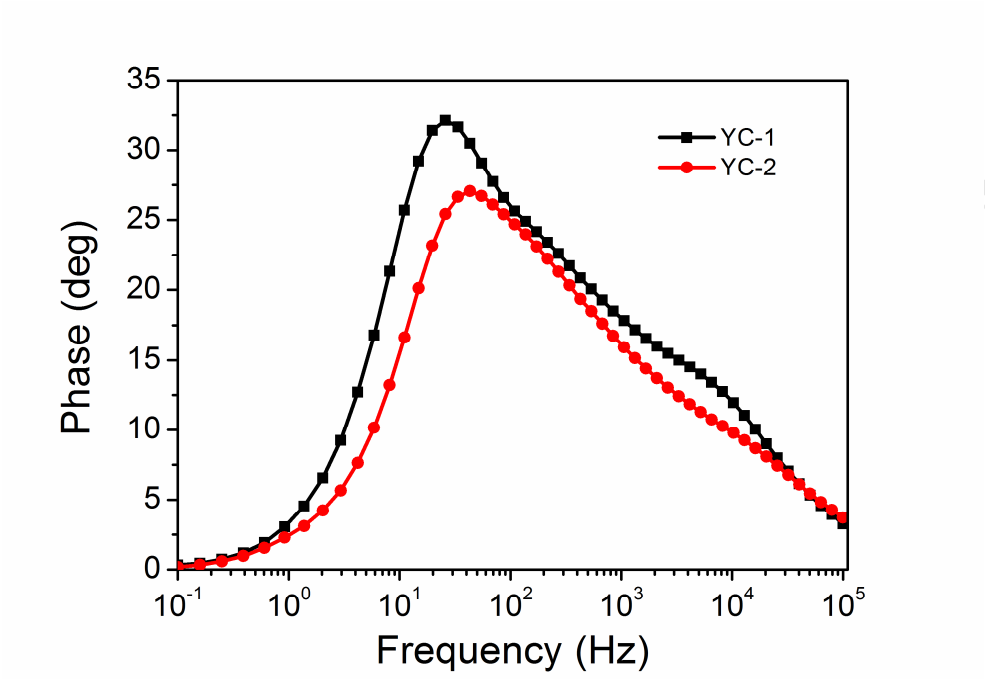

Research Highlights

- Tow D-π-A-π-A dyes bearing 5-phenyl-5H-dibenzo-[b,f]azepine units were synthesized.
- The effect of donor size on the property of sensitizer was systematically studied
- The dyes show panchromatic absorption between 300-800 nm in solution and neat film
- PCE of 4.38% was achieved for DSSCs based on I_3^-/I^- electrolyte without co-sensitizer